

## Observational constraints on the chemistry of isoprene nitrates over the eastern United States

Larry W. Horowitz,<sup>1</sup> Arlene M. Fiore,<sup>1</sup> George P. Milly,<sup>1</sup> Ronald C. Cohen,<sup>2</sup> Anne Perring,<sup>2</sup> Paul J. Wooldridge,<sup>2</sup> Peter G. Hess,<sup>3</sup> Louisa K. Emmons,<sup>3</sup> and Jean-François Lamarque<sup>3</sup>

Received 4 July 2006; revised 17 January 2007; accepted 5 February 2007; published 8 May 2007.

[1] The formation of organic nitrates during the oxidation of the biogenic hydrocarbon isoprene can strongly affect boundary layer concentrations of ozone and nitrogen oxides ( $\text{NO}_x = \text{NO} + \text{NO}_2$ ). We constrain uncertainties in the chemistry of these isoprene nitrates using chemical transport model simulations in conjunction with observations over the eastern United States from the International Consortium for Atmospheric Research on Transport and Transformation (ICARTT) field campaign during summer 2004. The model best captures the observed boundary layer concentrations of organic nitrates and their correlation with ozone using a 4% yield of isoprene nitrate production from the reaction of isoprene hydroxyperoxy radicals with  $\text{NO}$ , a recycling of 40%  $\text{NO}_x$  when isoprene nitrates react with  $\text{OH}$  and ozone, and a fast dry deposition rate of isoprene nitrates. Simulated boundary layer concentrations are only weakly sensitive to the rate of photochemical loss of the isoprene nitrates. An 8% yield of isoprene nitrates degrades agreement with the observations somewhat, but concentrations are still within 50% of observations and thus cannot be ruled out by this study. Our results indicate that complete recycling of  $\text{NO}_x$  from the reactions of isoprene nitrates and slow rates of isoprene nitrate deposition are incompatible with the observations. We find that  $\sim 50\%$  of the isoprene nitrate production in the model occurs via reactions of isoprene (or its oxidation products) with the  $\text{NO}_3$  radical, but note that the isoprene nitrate yield from this pathway is highly uncertain. Using recent estimates of rapid reaction rates with ozone, 20–24% of isoprene nitrates are lost via this pathway, implying that ozonolysis is an important loss process for isoprene nitrates. Isoprene nitrates are shown to have a major impact on the nitrogen oxide ( $\text{NO}_x = \text{NO} + \text{NO}_2$ ) budget in the summertime U.S. continental boundary layer, consuming 15–19% of the emitted  $\text{NO}_x$ , of which 4–6% is recycled back to  $\text{NO}_x$  and the remainder is exported as isoprene nitrates (2–3%) or deposited (8–10%). Our constraints on reaction rates, branching ratios, and deposition rates need to be confirmed through further laboratory and field measurements. The model systematically underestimates free tropospheric concentrations of organic nitrates, indicating a need for future investigation of the processes controlling the observed distribution.

**Citation:** Horowitz, L. W., A. M. Fiore, G. P. Milly, R. C. Cohen, A. Perring, P. J. Wooldridge, P. G. Hess, L. K. Emmons, and J.-F. Lamarque (2007), Observational constraints on the chemistry of isoprene nitrates over the eastern United States, *J. Geophys. Res.*, 112, D12S08, doi:10.1029/2006JD007747.

### 1. Introduction

[2] Photochemical oxidation of volatile organic compounds (VOCs) in the presence of nitrogen oxides ( $\text{NO}_x =$

$\text{NO} + \text{NO}_2$ ) contributes to the production of ozone. Over the eastern United States during summer, chemical reactivity and subsequent ozone production are dominated by isoprene (2-methyl-1, 3-butadiene), an abundant biogenic VOC that reacts rapidly with  $\text{OH}$  [e.g., Trainer *et al.*, 1987]. Isoprene oxidation also modulates the partitioning and fate of reactive nitrogen within the continental boundary layer [e.g., Horowitz *et al.*, 1998; Houweling *et al.*, 1998].

[3] Recent modeling studies have demonstrated that ozone concentrations and reactive nitrogen partitioning are sensitive to uncertainties in the isoprene chemical oxidation pathways [Horowitz *et al.*, 1998; von Kuhlmann *et al.*,

<sup>1</sup>Geophysical Fluid Dynamics Laboratory, NOAA, Princeton, New Jersey, USA.

<sup>2</sup>Department of Chemistry, University of California, Berkeley, California, USA.

<sup>3</sup>Atmospheric Chemistry Division, National Center for Atmospheric Research, Boulder, Colorado, USA.

2004; Fiore *et al.*, 2005; Wu *et al.*, 2007]. Specific uncertainties include the magnitude and spatial distribution of isoprene emissions, the yield and fate of isoprene nitrates, and the fate of organic hydroperoxides. Previous studies suggest that surface ozone is only weakly sensitive to the uncertainties in organic hydroperoxides (up to 2–3 ppbv), while the choice of isoprene emissions inventory can have large local or regional effects (up to 15 ppbv ozone locally) [von Kuhlmann *et al.*, 2004; Fiore *et al.*, 2005]. We focus on the uncertainties in isoprene nitrate chemistry, which have been shown to affect surface ozone (by up to 10 ppbv) and NO<sub>x</sub> (by up to 10%) [Horowitz *et al.*, 1998; von Kuhlmann *et al.*, 2004; Fiore *et al.*, 2005]. We analyze chemical transport model simulations in conjunction with observations from the International Consortium for Atmospheric Research on Transport and Transformation (ICARTT) field campaign [Fehsenfeld *et al.*, 2006; Singh *et al.*, 2006] conducted in summer 2004 to constrain the uncertainties in isoprene nitrate chemistry and examine the implications of these constraints for the NO<sub>x</sub> budget and ozone concentrations over the eastern United States.

[4] When isoprene is oxidized by OH, six different isomeric hydroxyperoxy (RO<sub>2</sub>) radicals are formed (after the addition of O<sub>2</sub>). Under high-NO<sub>x</sub> conditions these radicals typically react with NO, forming primarily hydroxalkoxy (RO) radicals with a minor channel leading to the production of organic hydroxynitrates (RONO<sub>2</sub>, “isoprene nitrates”) [e.g., Chen *et al.*, 1998]. Laboratory studies have estimated the yield of isoprene nitrates from the RO<sub>2</sub>+NO reaction to range from 4.4% to 15% (Chen *et al.* [1998], Tuazon and Atkinson [1990] (corrected as discussed by Paulson *et al.* [1992]), Chuong and Stevens [2002], and Sprengnether *et al.* [2002]). Model studies have shown that tropospheric ozone production and surface concentrations are sensitive to the isoprene nitrate yield [von Kuhlmann *et al.*, 2004; Wu *et al.*, 2007].

[5] The oxidation of isoprene by NO<sub>3</sub>, which occurs primarily at night, leads to the production of another set of isoprene nitrates. This pathway proceeds by addition of NO<sub>3</sub> to one of the double bonds in isoprene followed by addition of O<sub>2</sub> to form nitrooxyalkyl peroxy radicals. These radicals can then either undergo subsequent reactions to form stable organic nitrates or decompose to release NO<sub>x</sub>; the relative amounts of organic nitrates versus released NO<sub>x</sub> are poorly known [e.g., Paulson and Seinfeld, 1992; Fan and Zhang, 2004]. The isoprene nitrates formed by the isoprene-NO<sub>3</sub> channel are expected to be aldehydic [Paulson and Seinfeld, 1992] or ketonic nitrates [Fan and Zhang, 2004], as opposed to the hydroxynitrates formed from the isoprene-OH channel. The importance of the NO<sub>3</sub> versus OH pathways for isoprene nitrate production is also uncertain, but modeling [von Kuhlmann *et al.*, 2004] and observational [Starn *et al.*, 1998] studies both suggest that the isoprene-NO<sub>3</sub> channel may be a major source of isoprene nitrates.

[6] Isoprene nitrates contain a double bond, so they are highly reactive toward OH, ozone, and NO<sub>3</sub>. Reaction with OH is expected to be the major chemical loss [e.g., Shepson *et al.*, 1996]. Estimates of the reaction rate constant for isoprene nitrates + OH range from (1.3–9) × 10<sup>-11</sup> molecule<sup>-1</sup> cm<sup>3</sup> s<sup>-1</sup> [Paulson and Seinfeld, 1992; Shepson *et al.*, 1996; Chen

*et al.*, 1998; Giacomelli *et al.*, 2005], although some model studies have assumed rate constants as low as 6.8 × 10<sup>-13</sup> [Brasseur *et al.*, 1998]. Giacomelli *et al.* [2005] estimate a rate constant for isoprene nitrates + ozone of 1.33 × 10<sup>-17</sup> for terminally double-bonded isomers and a much faster rate constant of 4.03 × 10<sup>-16</sup> for internally double-bonded isomers, based on previous estimates for structurally similar alkenes. These rate constants correspond to a wide range in the lifetime of isoprene nitrates versus reaction with ozone (at 40 ppb ozone), from ~40 min. (for internally double-bonded isomers) to ~20 hours (for terminally bonded isomers). Previous modeling studies have used rate constants as low as 2.25 × 10<sup>-18</sup> by analogy with the rate constants for methylvinyl ketone and methacrolein [e.g., Horowitz *et al.*, 1998], or have neglected this reaction entirely [e.g., Pöschl *et al.*, 2000].

[7] The products of the isoprene nitrate chemical reactions have not been directly measured. Paulson and Seinfeld [1992] suggested that reaction with OH should release NO<sub>x</sub>, while other studies conclude that the reaction of some isomers will lead to the production of secondary multifunctional organic nitrates [Grossenbacher *et al.*, 2001; Giacomelli *et al.*, 2005]. The release of NO<sub>x</sub> by this reaction or its continued sequestration in organic nitrates can significantly alter the extent to which isoprene chemistry acts as a sink for NO<sub>x</sub> [e.g., Chen *et al.*, 1998; Horowitz *et al.*, 1998], with up to ~10% effects on surface ozone concentrations [von Kuhlmann *et al.*, 2004; Fiore *et al.*, 2005]. The efficiency of NO<sub>x</sub> recycling from the reactions of isoprene nitrates with ozone and NO<sub>3</sub> is also poorly known.

[8] Removal of isoprene nitrates by wet and dry deposition provides a permanent sink for atmospheric NO<sub>x</sub>. The rate of wet deposition depends on the Henry's law constant, which has been estimated by analogy with comparable species to range from H (298 K) = 6.0 × 10<sup>3</sup> M atm<sup>-1</sup> [Shepson *et al.*, 1996] to 1.7 × 10<sup>4</sup> [von Kuhlmann *et al.*, 2004]. Estimates of the dry deposition velocity of isoprene nitrates range from that of PAN (0.4–0.65 cm s<sup>-1</sup>) [Shepson *et al.*, 1996; Giacomelli *et al.*, 2005] to that of HNO<sub>3</sub> (4–5 cm s<sup>-1</sup>) [Rosen *et al.*, 2004; Hori *et al.*, 2006]. Using the slower deposition estimates and an OH rate constant of 1.3 × 10<sup>-11</sup> molecule<sup>-1</sup> cm<sup>3</sup> s<sup>-1</sup>, Shepson *et al.* [1996] predicted that reaction with OH should dominate over deposition, yielding overall atmospheric lifetime of ~18 hours (note that the reaction of isoprene nitrates with ozone was neglected in that study).

[9] The ICARTT multiagency international field campaign conducted during summer 2004 included measurements of isoprene, its oxidation products, reactive nitrogen compounds, and ozone over the eastern United States. Since chemistry in this region and season is strongly influenced by emissions of both biogenic isoprene and anthropogenic NO<sub>x</sub>, the ICARTT campaign presents an opportunity to study the effect of isoprene on reactive nitrogen partitioning and ozone production. We analyze the ICARTT observations in conjunction with a three-dimensional chemical transport model to identify new constraints on the chemistry of isoprene nitrates. The model is described in section 2 and evaluated with observations in section 3. In section 4, we examine the sensitivity of our results to uncertainties in isoprene nitrate chemistry, derive observational constraints on this chemistry, and discuss the implications for the NO<sub>x</sub>

**Table 1.** Isoprene and Monoterpene Mechanism Used in Base Model Simulations<sup>a</sup>

Reaction	Rate Constant
ISOP + OH → ISOPO2	2.54E-11*exp(410/T)
ISOP + O3 → 0.4*MACR + 0.2*MVK + 0.07*C3H6 + 0.27*OH + 0.06*HO2 + 0.6*CH2O + 0.3*CO + 0.1*O3 + 0.2*MCO3 + 0.2*CH3COOH	1.05E-14*exp(-2000/T)
ISOP + NO3 → ISOPNO3	3.03E-12*exp(-446/T)
ISOPO2 + NO → 0.04*ONITR + 0.96*NO2 + HO2 + 0.57*CH2O + 0.24*MACR + 0.33*MVK + 0.38*HYDRALD	2.20E-12*exp(180/T)
ISOPO2 + NO3 → HO2 + NO2 + 0.6*CH2O + 0.25*MACR + 0.35*MVK + 0.4*HYDRALD	2.40E-12
ISOPO2 + HO2 → ISOPOOH	8.00E-13*exp(700/T)
ISOPO2 + CH3O2 → 0.25*CH3OH + HO2 + 1.2*CH2O + 0.19*MACR + 0.26*MVK + 0.3*HYDRALD	5.00E-13*exp(400/T)
ISOPO2 + CH3CO3 → CH3O2 + HO2 + 0.6*CH2O + 0.25*MACR + 0.35*MVK + 0.4*HYDRALD	1.40E-11
MVK + hv → 0.7*C3H6 + 0.7*CO + 0.3*CH3O2 + 0.3*CH3CO3	photolysis
MVK + OH → MACRO2	4.13E-12*exp(452/T)
MVK + O3 → 0.8*CH2O + 0.95*CH3COCHO + 0.08*OH + 0.2*O3 + 0.06*HO2 + 0.05*CO + 0.04*CH3CHO	7.52E-16*exp(-1521/T)
MACR + hv → 0.67*HO2 + 0.33*MCO3 + 0.67*CH2O + 0.67*CH3CO3 + 0.33*OH + 0.67*CO	photolysis
MACR + OH → 0.5*MACRO2 + 0.5*H2O + 0.5*MCO3	1.86E-11*exp(175/T)
MACR + O3 → 0.8*CH3COCHO + 0.275*HO2 + 0.2*CO + 0.2*O3 + 0.7*CH2O + 0.215*OH	4.40E-15*exp(-2500/T)
MACRO2 + NO → NO2 + 0.47*HO2 + 0.25*CH2O + 0.25*CH3COCHO + 0.53*CH3CO3 + 0.53*GLYALD + 0.22*HYAC + 0.22*CO	2.70E-12*exp(360/T)
MACRO2 + NO → ONITR	1.30E-13*exp(360/T)
MACRO2 + NO3 → NO2 + 0.47*HO2 + 0.25*CH2O + 0.25*CH3COCHO + 0.22*CO + 0.53*GLYALD + 0.22*HYAC + 0.53*CH3CO3	2.40E-12
MACRO2 + HO2 → MACROOH	8.00E-13*exp(700/T)
MACRO2 + CH3O2 → 0.73*HO2 + 0.88*CH2O + 0.11*CO + 0.24*CH3COCHO + 0.26*GLYALD + 0.26*CH3CO3 + 0.25*CH3OH + 0.23*HYAC	5.00E-13*exp(400/T)
MACRO2 + CH3CO3 → 0.25*CH3COCHO + CH3O2 + 0.22*CO + 0.47*HO2 + 0.53*GLYALD + 0.22*HYAC + 0.25*CH2O + 0.53*CH3CO3	1.40E-11
ISOPOOH + hv → 0.402*MVK + 0.288*MACR + 0.69*CH2O + HO2	photolysis
ISOPOOH + OH → 0.5*XO2 + 0.5*ISOPO2	3.80E-12*exp(200/T)
MACROOH + OH → 0.5*MCO3 + 0.2*MACRO2 + 0.1*OH + 0.2*HO2	2.30E-11*exp(200/T)
ONITR + hv → HO2 + CO + NO2 + CH2O	photolysis
ONITR + OH → 0.4*HYDRALD + 0.4*NO2 + HO2 + 0.6*XNITR	4.50E-11
ONITR + O3 → 0.4*HYDRALD + 0.4*NO2 + HO2 + 0.6*XNITR	1.30E-16
ONITR + NO3 → NO2 + HO2 + XNITR	1.40E-12*exp(-1860/T)
ISOPNO3 + NO → 1.206*NO2 + 0.794*HO2 + 0.072*CH2O + 0.167*MACR + 0.039*MVK + 0.794*ONITR	2.70E-12*exp(360/T)
ISOPNO3 + NO3 → 1.206*NO2 + 0.072*CH2O + 0.167*MACR + 0.039*MVK + 0.794*ONITR + 0.794*HO2	2.40E-12
ISOPNO3 + HO2 → 0.206*NO2 + 0.794*HO2 + 0.008*CH2O + 0.167*MACR + 0.039*MVK + 0.794*ONITR	8.00E-13*exp(700/T)
C10H16 + OH → TERPO2	1.20E-11*exp(444/T)
C10H16 + O3 → 0.7*OH + MVK + MACR + HO2	1.00E-15*exp(-732/T)
C10H16 + NO3 → TERPO2 + NO2	1.20E-12*exp(490/T)
TERPO2 + NO → 0.1*CH3COCH3 + HO2 + 0.82*MVK + 0.82*MACR + 0.82*NO2 + 0.18*ONITR	4.20E-12*exp(180/T)
TERPO2 + HO2 → TERPOOH	7.50E-13*exp(700/T)
TERPOOH + hv → OH + 0.1*CH3COCH3 + HO2 + MVK + MACR	photolysis
TERPOOH + OH → TERPO2	3.80E-12*exp(200/T)

<sup>a</sup>Second-order reaction rate constants are given in units of molecule<sup>-1</sup> cm<sup>3</sup> s<sup>-1</sup>.

budget over the eastern United States. Conclusions are presented in section 5.

## 2. Model Description

[10] We simulate the chemistry during the ICARTT period (July–August 2004) using the Model of Ozone and Related Chemical Tracers, version 4 (MOZART-4) chemical transport model [Emmons *et al.*, 2006; L. Emmons *et al.*, manuscript in preparation, 2007]. This model is an updated version of the MOZART-2 model [Horowitz *et al.*, 2003] with aerosol chemistry based on that of Tie *et al.* [2005]. In MOZART-4, photolysis rates are calculated interactively using Fast-TUV to account for absorption and scattering by aerosols and clouds [Madronich and Flocke, 1998; Tie *et al.*, 2005]. The influx of O<sub>3</sub> from the stratosphere is prescribed using the SYNOZ technique (500 Tg yr<sup>-1</sup>) [McLinden *et al.*, 2000]. The prescribed monthly mean deposition velocities for O<sub>3</sub> and PAN have been increased following Bey *et al.* [2001], although a recent observational study suggests that the PAN deposition velocities may still be underestimated [Turnipseed *et al.*, 2006]. The mechanism now represents the chemistry of higher alkanes with

the “bigalk” (C<sub>5</sub>H<sub>12</sub>) tracer, a lumped species representing the butanes, pentanes, and hexanes. Higher alkenes are included as “bigene” (C<sub>4</sub>H<sub>8</sub>), a lumped species representing mostly 2-methylpropene and 2-butene. An additional new species, “toluene” (C<sub>7</sub>H<sub>8</sub>), is a lumped aromatic compound representing mostly benzene, toluene, and the xylenes. Additional oxidation products of the above species have also been added. Updates to the chemistry in MOZART-4 are more fully described by Emmons *et al.* (manuscript in preparation, 2007).

[11] The isoprene and monoterpene oxidation mechanisms in our BASE simulation are shown in Table 1. In section 4, we evaluate the sensitivity of our results to the assumptions in our BASE isoprene mechanism described here, using the additional model simulations described in Table 2. The treatment of isoprene nitrates has been modified from that in MOZART-2 [Horowitz *et al.*, 2003]. The yield of ONITR from the addition branch of the ISOPO2 + NO reaction has been decreased from 8% in MOZART-2 to 4% [e.g., Chen *et al.*, 1998] in the BASE simulation. A new species (XNITR in Table 1) represents secondary multifunctional organic nitrates. The reaction of primary isoprene

**Table 2.** Sensitivity Simulations in MOZART-4 Model

Simulation	Yield <sup>a</sup>	Loss Rate <sup>b</sup>	Deposition <sup>c</sup>	NO <sub>x</sub> Recycling <sup>d</sup>	Isoprene Nitrate Burden, <sup>e</sup> GgN	Isoprene Nitrate Lifetime, <sup>f</sup> hours
4% (BASE)	4%	fast	fast	40%	1.46	13.8
4%_slowCHEM	4%	slow	fast	40%	1.53	14.5
4%_slowDD	4%	fast	slow	40%	3.03	28.5
8%	8%	fast	fast	40%	1.82	14.0
8%_slowCHEM	8%	slow	fast	40%	1.91	14.8
8%_slowDD	8%	fast	slow	40%	3.76	28.9
4%_0%NOx	4%	fast	fast	0%	2.27	22.2
4%_100%NOx	4%	fast	fast	100%	0.13	1.1
8%_slowCHEM_100%NOx	8%	slow	fast	100%	0.36	2.7

<sup>a</sup>Yield of isoprene nitrates (ONITR) from the reaction of isoprene peroxy radicals (ISOP2) with NO.

<sup>b</sup>Loss rates of ONITR. “Fast” indicates  $k(\text{ONITR} + \text{OH}) = 4.5 \times 10^{-11} \text{ molecule}^{-1} \text{ cm}^3 \text{ s}^{-1}$ ,  $k(\text{ONITR} + \text{O}_3) = 1.30 \times 10^{-16}$ ,  $J(\text{ONITR}) = J(\text{CH}_3\text{CHO})$ . “Slow” indicates  $k(\text{ONITR} + \text{OH}) = 1.3 \times 10^{-11}$ ,  $k(\text{ONITR} + \text{O}_3) = 4.33 \times 10^{-17}$ ,  $J(\text{ONITR}) = J(\text{HNO}_3)$ .

<sup>c</sup>Rate of ONITR (and XNITR) dry deposition. “Fast” indicates  $V_d(\text{ONITR}) = V_d(\text{HNO}_3)$ . “Slow” indicates  $V_d(\text{ONITR}) = V_d(\text{PAN})$ . In both cases, wet deposition is based on a Henry’s Law constant of  $H_{298}(\text{ONITR}) = 7.51 \times 10^3 \text{ M atm}^{-1}$ .

<sup>d</sup>Recycling of NO<sub>x</sub> from reactions of ONITR with OH and ozone. The balance of the reactive nitrogen produces multifunctional organic nitrates (XNITR).

<sup>e</sup>Mean burden of isoprene nitrates (ONITR + XNITR + ISOPNO3) in the eastern United States (24–52°N, 62.5–97.5°W) boundary layer (below 800 hPa) during July 2004.

<sup>f</sup>Mean lifetime of isoprene nitrates (ONITR + XNITR + ISOPNO3) in the eastern United States boundary layer during July 2004 versus all loss processes shown in Figure 2.

nitrates (ONITR) with OH recycles 40% of NO<sub>x</sub>, rather than 100% as in MOZART-2, with the balance forming XNITR based on recent studies suggesting that this reaction produces some secondary nitrates [e.g., *Grossenbacher et al.*, 2001; *Giacopelli et al.*, 2005]. XNITR is removed by wet and dry deposition at the same rates as ONITR, but has no chemical losses in our mechanism, as its further reactions are assumed to convert it to more highly substituted organic nitrates. The reaction ONITR + ozone has been added with a reaction rate constant based on a weighted average of the values recommended by *Giacopelli et al.* [2005], with the same products as the ONITR + OH reaction. The reaction ONITR + NO<sub>3</sub> is also assumed to produce XNITR. Note that the carbonyl nitrates produced from the isoprene-NO<sub>3</sub> channel (via ISOPNO3) are represented in our mechanism by the same ONITR species as the hydroxynitrates from the isoprene-OH channel. This simplifying assumption neglects any differences in reactivity or deposition between these two different classes of isoprene nitrates.

[12] The oxidation scheme for monoterpenes, represented by  $\alpha$ -pinene, has been updated to reflect recent laboratory data (see Table 1 and Emmons et al. (manuscript in preparation, 2007)). We assume that terpene oxidation produces organic nitrates with an 18% yield from the reaction of terpene peroxy radicals (TERPO2) with NO [*Nozière et al.*, 1999]. We note that this yield is considerably higher than the  $\sim 1\%$  yield estimated by *Aschmann et al.* [2002], although *Aschmann et al.* acknowledged the possibility that their results were biased low by aerosol formation or loss to the chamber wall.

[13] Global anthropogenic, biomass burning, and natural emissions were updated from those used by *Horowitz et al.* [2003] based on the POET emissions inventory for 1997 [*Olivier et al.*, 2003; <http://www.aero.jussieu.fr/projet/ACCENT/POET.php>]. Isoprene and monoterpene emissions are calculated interactively as a function of temperature, sunlight, and vegetation type using algorithms from the Model of Emissions of Gases and Aerosols from Nature (MEGAN v.0) [*Guenther et al.*, 2006]. Over North America during summer, we use updated anthropogenic surface

emissions based on the EPA National Emissions Inventory (NEI99, version 3, <http://www.epa.gov/ttn/chieff/net/1999inventory.html>) (S. McKeen, personal communication, 2004), and the daily biomass burning emission inventory developed by *Turquety et al.* [2007]. Biomass burning emissions are distributed vertically up to 4 km altitude, with 70% of the emissions occurring below 2 km. Surface emissions over the eastern United States (24–52°N, 62.5–97.5°W) in July 2004 total 0.52 TgN NO<sub>x</sub>, 7.8 Tg CO, 3.7 TgC isoprene, and 0.91 TgC terpenes.

[14] Meteorological fields are provided by the NCEP Global Forecast System (GFS) every three hours. The model resolution is 1.9° latitude  $\times$  1.9° longitude, with 64 vertical levels and a dynamical and chemical time step of 15 min. The BASE model simulation was conducted from December 2003 through the ICARTT period (July–August 2004). Sensitivity simulations (section 4.1) begin in May 2004, allowing for a 2-month spin-up period sufficient to capture changes in summertime continental boundary layer chemistry.

### 3. Results From Base Simulation

#### 3.1. Evaluation With ICARTT Observations

[15] We evaluate the results of the MOZART-4 BASE simulation with observations made on board the NASA DC-8 [*Singh et al.*, 2006] and NOAA WP-3D [*Fehsenfeld et al.*, 2006] aircraft during ICARTT. Simulated concentrations are sampled every minute along the flight tracks of the two aircraft and then averaged onto the model grid for each flight. The two aircraft pursued different sampling strategies: the DC-8, based in St. Louis, Missouri and Portsmouth, New Hampshire, typically aimed to sample regionally representative air masses; the WP-3D, based in Portsmouth, New Hampshire often sampled local plumes from urban outflow or power plants. (See ICARTT overview papers [*Fehsenfeld et al.*, 2006; *Singh et al.*, 2006] for more details about the aircraft flight tracks.)

[16] Comparisons of selected species, including isoprene, isoprene oxidation products, ozone, and ozone precursors, below 2 km in the eastern United States are presented in

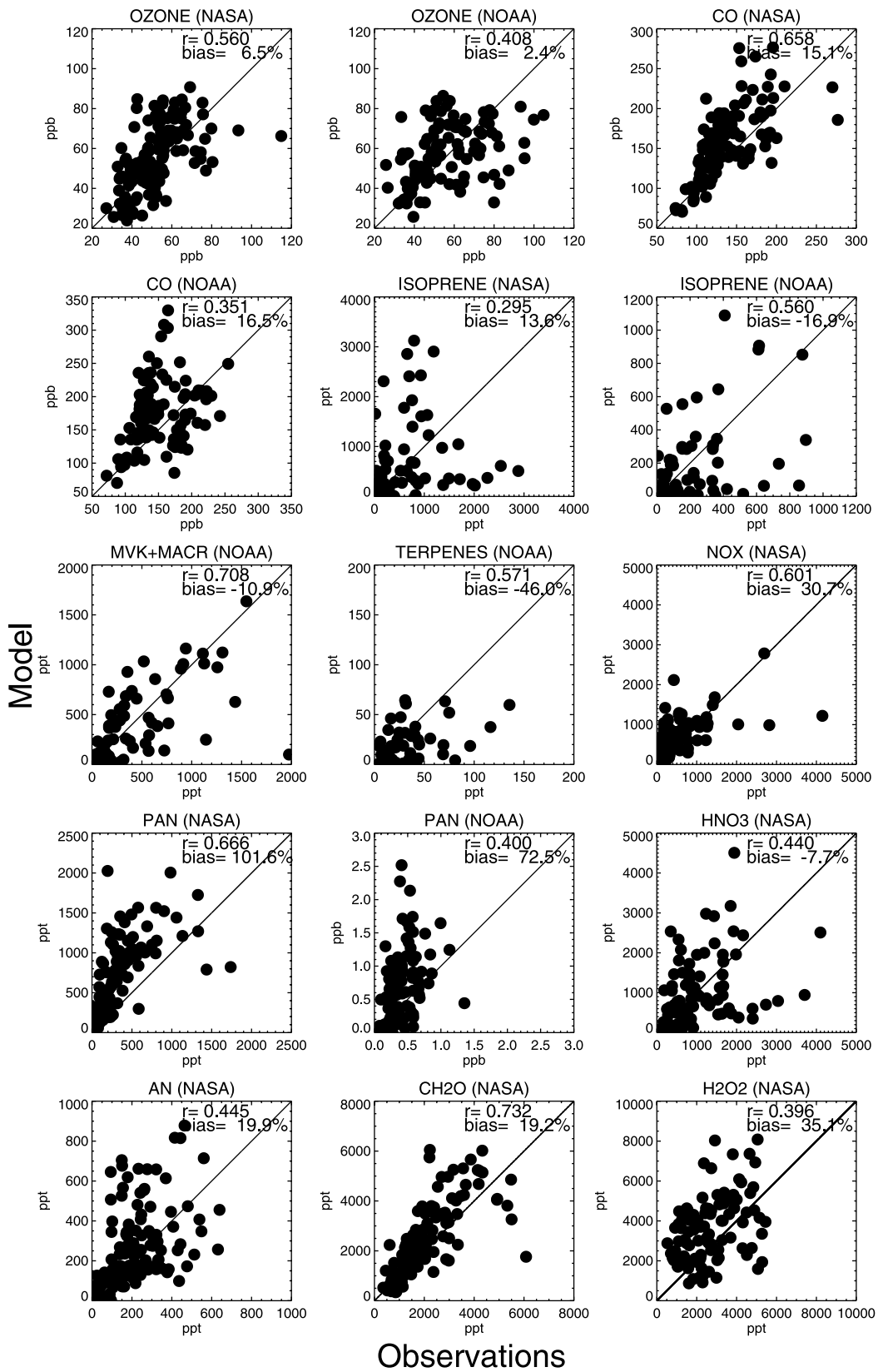


Figure 1

Figure 1. Isoprene concentrations show little bias, but are poorly correlated with observations ( $r^2 = 0.09$  and mean bias = +14% for NASA,  $r^2 = 0.31$  and bias = -17% for NOAA), most likely because of the short lifetime of isoprene and the high spatial variability of its emissions. The first generation isoprene oxidation products methylvinyl ketone and methacrolein, which have longer atmospheric lifetimes, are better simulated by the model ( $r^2 = 0.50$ , bias = -11%). Monoterpene concentrations are underestimated by almost a factor of 2, but correlated with observations ( $r^2 = 0.33$ ). Overall, we conclude that the MEGAN biogenic emission inventory captures the magnitude and large-scale spatial pattern of isoprene emissions, but may underestimate terpene emissions.

[17] Boundary layer concentrations of ozone are slightly overestimated (mean bias = +6.5% for NASA, +2.4% for NOAA) and moderately correlated with observations ( $r^2 = 0.31$  for NASA, 0.17 for NOAA). CO and NO<sub>x</sub> are moderately well correlated with observations ( $r^2 = 0.43$  and 0.12 for CO from NASA and NOAA, respectively,  $r^2 = 0.36$  for NO<sub>x</sub> from NASA), with an average model overestimate of ~15% for CO and ~30% for NO<sub>x</sub>. The model overestimate of NO<sub>x</sub> concentrations can be attributed to our use of the NEI99 emission inventory (for the year 1999), which overestimates the power plant emissions of NO<sub>x</sub> during 2004 [Frost *et al.*, 2006]. The lower correlations of our results with the NOAA measurements are expected as a result of the poor representation of the local plumes sampled by the WP-3D in our coarse resolution model. Secondary oxidation products PAN and formaldehyde (CH<sub>2</sub>O) are well correlated with the observations, but PAN tends to be overestimated in the boundary layer. PAN concentrations in the free troposphere have little mean bias (not shown). Simulated organic nitrates (ONITR + XNITR + ISOPNO<sub>3</sub> + other organic nitrates) are overestimated in the mean (+20%) versus the observed total alkyl- and hydroxyalkyl-nitrates (ΣANs) [Day *et al.*, 2002] (bias = +20%) and are poorly correlated with the observations ( $r^2 = 0.20$ ). We found little systematic correlation between the errors in organic nitrates and those in the other species in Figure 1 (e.g., isoprene, NO<sub>x</sub>, PAN, CO). The small-scale errors in isoprene emissions mentioned above may contribute to errors in the organic nitrates on the same scales, since isoprene is the

major source of these nitrates (section 3.2). Concentrations of HNO<sub>3</sub> and H<sub>2</sub>O<sub>2</sub> are poorly correlated with observations, suggesting possible model errors in wet deposition.

[18] With the exception of organic nitrates, the agreement between simulated and observed concentrations for the species evaluated in Figure 1 is relatively insensitive to assumptions about isoprene nitrate chemistry (at least to within model biases), as represented by the sensitivity simulations in section 4.1. We thus use only the observed ΣAN concentrations to provide constraints on the chemistry of isoprene nitrates (section 4.2). We begin by examining the budget of isoprene nitrates in section 3.2.

### 3.2. Isoprene Nitrate Budget

[19] Budgets for isoprene nitrate (ONITR+XNITR+ISOPNO<sub>3</sub>) production and loss in the eastern United States (24–52°N, 62.5–97.5°W) boundary layer (below 800 hPa) during July 2004 are presented in Figure 2. In the BASE simulation, half of the isoprene nitrate production occurs through the NO<sub>3</sub> pathway, in which isoprene reacts with NO<sub>3</sub> to form ISOPNO<sub>3</sub>, which can then react with NO, NO<sub>3</sub>, or HO<sub>2</sub> to form carbonyl nitrates. These carbonyl nitrates, represented in our mechanism by the same ONITR species as the hydroxynitrates formed from the isoprene-OH pathway, are assumed to form with a yield of 79.4% from all ISOPNO<sub>3</sub> reaction pathways (see Table 1) [Horowitz *et al.*, 2003]. The large contribution of this pathway to isoprene nitrate production, despite the small fraction of isoprene oxidized via this pathway (~6%), agrees well with the findings of von Kuhlmann *et al.* [2004]. About 25% of the isoprene nitrate production occurs via the reaction ISOPO<sub>2</sub> + NO, which produces ONITR with a 4% yield in this simulation. Each of the reactions MACRO<sub>2</sub> + NO and TERPO<sub>2</sub> + NO (TERPO<sub>2</sub> is formed by terpenes + OH or terpenes + NO<sub>3</sub>) yields another 12–14%. This partitioning of organic nitrate sources is similar to that calculated by Cleary *et al.* [2005] for the suburbs of Sacramento, CA. Note that we assume the same ONITR yield from terpenes + OH and terpenes + NO<sub>3</sub> (18%), while in the case of isoprene we include a much higher yield from isoprene + NO<sub>3</sub> (79.4%) than for isoprene + OH (4% in the BASE case); the actual yield of organic nitrates from terpenes + NO<sub>3</sub> is likely to be considerably higher than the 18% yield assumed

**Figure 1.** MOZART-4 model versus observed concentrations of selected trace species for daytime observations (1500–2300 UTC) below 2 km in the eastern United States (24–52°N, 62.5–97.5°W). Hourly model results are sampled at the locations of 1-min observations. The 1-min model values and observations for each NOAA WP-3D and NASA DC-8 flight are then averaged onto the model grid. Observations shown from the NASA DC-8 are ozone (PI: Avery, chemiluminescence), CO (PI: Sachse differential absorption TDL spectrometer) [Sachse *et al.*, 1987; Vay *et al.*, 1998], isoprene (PI: D. Blake, whole-air sample, gas chromatography) [Blake *et al.*, 2003], NO<sub>x</sub> = NO (PI: Brune) (X. Ren *et al.*, HO<sub>x</sub> observation and model comparison during INTEX-NA 2004, submitted to *Journal of Geophysical Research*, 2007) + NO<sub>2</sub> (PI: Cohen, laser induced fluorescence) [Thornton *et al.*, 2000], PAN (PI: Singh, electron-capture gas chromatography) [Singh *et al.*, 2000, 2007], HNO<sub>3</sub> and H<sub>2</sub>O<sub>2</sub> (PI: Wennberg, chemical ionization mass spectrometer) [Crouse *et al.*, 2006], total alkyl- and hydroxyalkyl-nitrates (AN, PI: Cohen, thermal dissociation - laser induced fluorescence) [Day *et al.*, 2002; Cleary *et al.*, 2005], and CH<sub>2</sub>O (PI: Fried, TDLAS) [Roller *et al.*, 2006, and references therein]. Observations shown from the NOAA WP-3D are ozone (PI: Ryerson, chemiluminescence) [Ryerson *et al.*, 2003], CO (PI: Holloway, vacuum UV fluorescence) [Holloway *et al.*, 2000], isoprene, methylvinyl ketone + methacrolein (MVK+MACR), and monoterpenes (PIs: de Gouw and Warneke, PTR-MS) [de Gouw *et al.*, 2003, 2006], and PAN (PI: Flocke, thermal dissociation-chemical ionization mass spectrometry) [Slusher *et al.*, 2004].

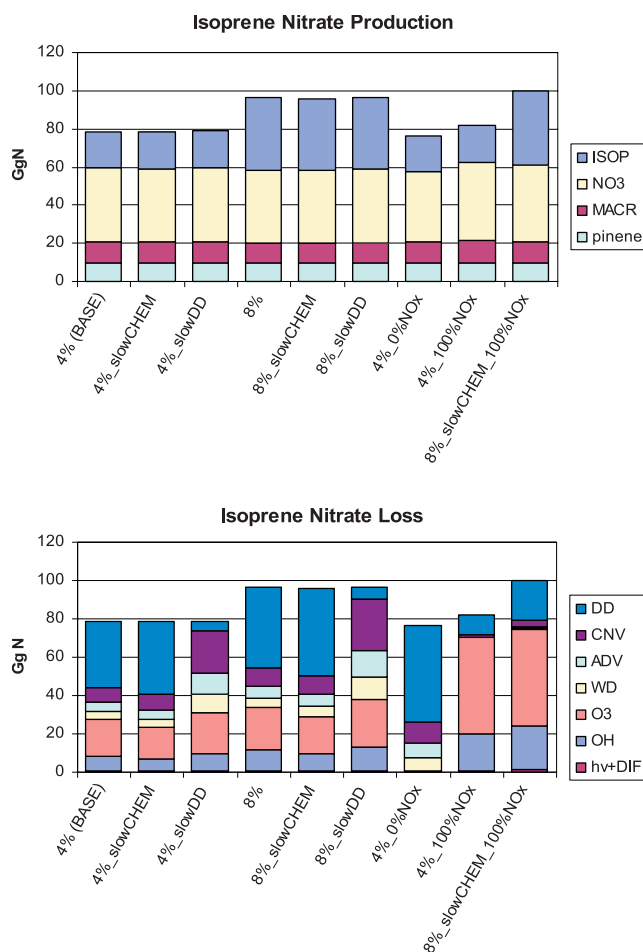


**Figure 2.** Budgets of isoprene nitrates (ONITR + XNITR + ISOPNO<sub>3</sub>) in the eastern United States (24–52°N, 62.5–97.5°W) boundary layer (below 800 hPa) during July 2004 for each model simulation. Production of isoprene nitrates occurs from terpenes (pinene), methylvinyl ketone and methacrolein (MACR), and from isoprene reactions with NO<sub>3</sub> (NO<sub>3</sub>) and OH (ISOP). Loss occurs via photolysis and vertical diffusion (hv + DIF), reaction with OH (OH) and ozone (O<sub>3</sub>), wet deposition (WD), advection (ADV), convection (CNV), and dry deposition (DD).

in our mechanism. The loss of isoprene nitrates in the BASE simulation occurs largely by dry deposition (44%) and reaction with ozone (24%) and OH (10%), with additional losses by transport (16%) and wet deposition (5%).

#### 4. Isoprene Nitrate Sensitivity Analysis

[20] In this section, we examine the sensitivity of our model results to assumptions concerning the production and loss of isoprene nitrates, using the additional simulations in Table 2. In particular, we examine the sensitivity of isoprene nitrates to the assumed yield, OH reaction rate, recycling of NO<sub>x</sub>, and deposition rate. We place constraints on the isoprene nitrate chemistry based on boundary layer observations of ΣAN, and quantify the effects of isoprene nitrates on the NO<sub>x</sub> budget over the eastern United States.

#### 4.1. Sensitivity Simulations

[21] The production of isoprene nitrates following the oxidation of isoprene by OH depends on the yield of these nitrates from the reaction of the isoprene peroxy radicals (ISOPO<sub>2</sub> in Table 1) with NO. We conduct sensitivity simulations in which the yield is increased from the BASE case value of 4% [Chen *et al.*, 1998] to 8%, as assumed by Fan and Zhang [2004]. In the simulations with an 8% yield (8% and 8%\_slowCHEM in Table 2), the production of isoprene nitrates via the ISOPO<sub>2</sub>+NO pathway doubles compared to the runs with a 4% yield (BASE and 4%\_slowCHEM), but production via other pathways is relatively unchanged (Figure 2). Thus the total production of isoprene nitrates increases by 23% in these simulations.

[22] The chemical loss of isoprene nitrates (ONITR) is primarily through reaction with ozone (~70% in the BASE case), followed by reaction with OH. We test here the effects of slower photochemical loss of isoprene nitrates, as applied in earlier studies. Our BASE simulation assumes a rate constant of  $k = 4.5 \times 10^{-11}$  molecule<sup>-1</sup> cm<sup>3</sup> s<sup>-1</sup> for isoprene nitrates + OH (Emmons *et al.*, manuscript in preparation, 2007), within the range of (3–9) × 10<sup>-11</sup> molecule<sup>-1</sup> cm<sup>3</sup> s<sup>-1</sup> estimated by Giacomelli *et al.* [2005] using the method of Kwok and Atkinson [1995]. There is evidence that the Kwok and Atkinson [1995] method may overestimate the rate constant for OH reaction with hydroxalkyl nitrates by a factor of 2–21 [Neeb, 2000; Treves and Rudich, 2003], so we also consider a lower rate constant of  $k = 1.3 \times 10^{-11}$  molecule<sup>-1</sup> cm<sup>3</sup> s<sup>-1</sup> (simulations 4%\_slowCHEM, 8%\_slowCHEM), similar to that used in several other studies [Shepson *et al.*, 1996; Chen *et al.*, 1998; Pöschl *et al.*, 2000; Horowitz *et al.*, 2003]. In these simulations, we also decrease the rate of the isoprene nitrates + ozone reaction by a factor of 3 from its BASE case value of  $k = 1.30 \times 10^{-16}$  and decrease the photolysis rate for ONITR, J(ONITR), from its BASE case value of J(CH<sub>3</sub>CHO) to J(HNO<sub>3</sub>). The ONITR reactions with ozone and OH together account for 34% of the isoprene nitrate loss when a fast reaction rate is assumed (BASE and 8%), but only 29% when a slower rate is used (4%\_slowCHEM and 8%\_slowCHEM in Figure 2). Photolysis of ONITR is a minor loss in all simulations, accounting for 1% or less of the isoprene nitrate loss in all simulations. The overall lifetime of isoprene nitrates (ONITR+XNITR+ISOPNO<sub>3</sub>) increases by only 5% in the simulations with slower ONITR photochemical loss (Table 2).

[23] When isoprene nitrates (ONITR) react with ozone and OH, the reactive nitrogen can be recycled to NO<sub>x</sub> or retained as XNITR. In the BASE case, we assume a NO<sub>x</sub> recycling efficiency of 40%. Since this recycling efficiency is uncertain [Paulson and Seinfeld, 1992; Chen *et al.*, 1998; Grossenbacher *et al.*, 2001; Giacomelli *et al.*, 2005], we include three sensitivity simulations in which the recycling is varied from extreme values of 0% (4%\_0%NO<sub>x</sub> in Table 2) to 100% (4%\_100%NO<sub>x</sub> and 8%\_slowCHEM\_100%NO<sub>x</sub>). When the recycling is completely turned off, the ONITR reactions with ozone and OH cease to be sinks for isoprene nitrates and instead produce 100% XNITR. As a result, the burden of isoprene nitrates increases by 56% (Table 2) and losses via dry and wet deposition increase by 43% and 60%, respectively (Figure 2). When the recycling is increased from 40% to

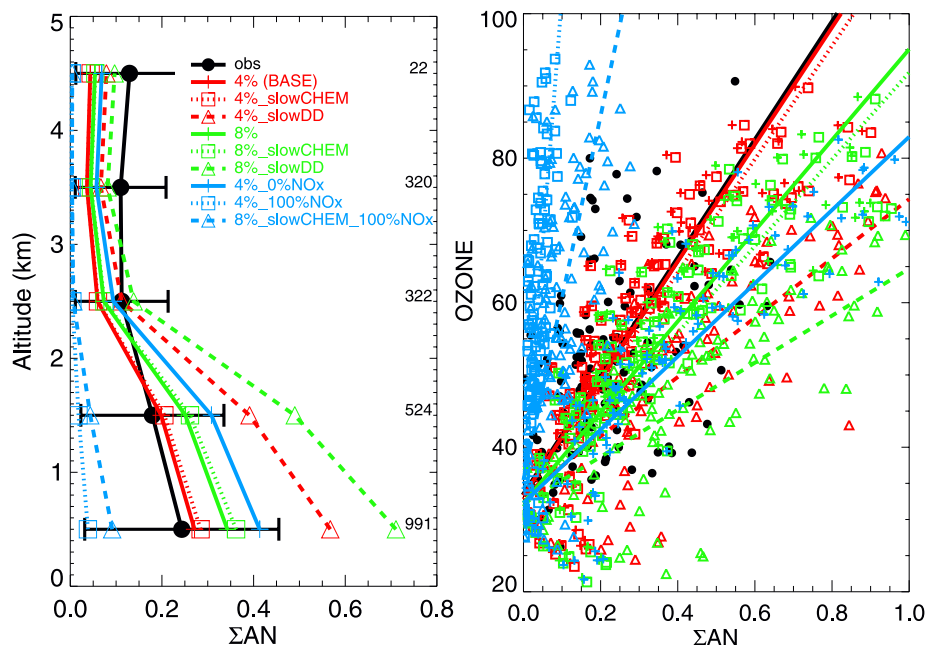


**Figure 3.** (left) Mean ICARTT vertical profile of the sum of all alkyl nitrates ( $\Sigma\text{AN}$ ) from observations (black; standard deviations indicated by horizontal bars) and model (colored by simulation as shown in legend; see also Table 2) from all DC-8 flights. (right) Correlation plot of ozone versus  $\Sigma\text{AN}$  and reduced major axis regression line from observations (black points and line) and model (colored points and lines) for daytime (1500–2300 UTC) DC-8 data over the eastern United States (24–52°N, 62.5–97.5°W). Hourly model results are sampled at the locations of the 1-min observations. In the ozone- $\Sigma\text{AN}$  correlation plot, 1-min data points for each flight have been averaged onto the model grid.

100%, the losses of isoprene nitrates from the ONITR reactions with ozone and OH increase nearly proportionally by a factor of 2.6 to account together for 73–85% of the total loss, causing the isoprene nitrate burden and lifetime to decrease by a factor of 5–12.

[24] The final sensitivity we examine is the rate at which isoprene nitrates (ONITR and XNITR) are lost by deposition. In the BASE simulation, we assume that isoprene nitrates deposit rapidly, with a dry deposition velocity equal to that of  $\text{HNO}_3$  and a wet deposition rate (Henry’s Law constant of  $\text{H}_{298} = 7.51 \times 10^3 \text{ M atm}^{-1}$ ) similar to that assumed by Shepson *et al.* [1996]. Since dry deposition dominates over wet deposition as a loss pathway from the boundary layer (see section 3.2 and Figure 2), we examine the sensitivity of our results to the removal rate by decreasing the dry deposition velocity of isoprene nitrates by a factor of  $\sim 20$  to that of PAN (simulations 4% slowDD, 8%\_slowDD) [Shepson *et al.*, 1996; Giacomelli *et al.*, 2005]. In these simulations with slow dry deposition, the isoprene nitrate burden and lifetime increase by a factor of 2 (Table 2) and export and chemical loss of ONITR by increase in importance, accounting for 43% and 38% of the total loss, respectively (Figure 2).

#### 4.2. Constraints From Observations

[25] The sensitivity simulations described above (section 4.1 and Table 2) most dramatically affect the concentrations of isoprene nitrates, with only small impacts on the other species evaluated in section 3.1. Previous calculations have shown that biogenically derived nitrates are the primary source of  $\Sigma\text{ANs}$  in Sacramento [Cleary *et al.*, 2005],

in eastern Pennsylvania [Trainer *et al.*, 1991], rural Michigan and Alabama [Sillman and Samson, 1995], and rural Ontario [O’Brien *et al.*, 1995], but not in Houston, Texas [Rosen *et al.*, 2004]. The speciated (nonisoprene) alkyl nitrates measured from whole-air samples during ICARTT (by D. Blake) typically account for an average of only  $\sim 10\%$  of the observed  $\Sigma\text{ANs}$ , indicating that the  $\Sigma\text{ANs}$  are primarily composed of larger compounds or multifunctional compounds such as the isoprene and terpene nitrates, consistent with the model results. A more detailed discussion of the comparison of individually measured nitrates to the observations of  $\Sigma\text{ANs}$  is presented in a forthcoming paper by A. Perring *et al.* (manuscript in preparation). In this section, we utilize measurements of total alkyl- and hydroxyalkyl-nitrates ( $\Sigma\text{ANs}$ ) [Day *et al.*, 2002] during ICARTT to constrain the chemistry of isoprene nitrates.

[26] Simulated organic nitrate concentrations (ONITR + XNITR + ISOPNO<sub>3</sub> + other organic nitrates) are compared with observations of  $\Sigma\text{ANs}$  in Figure 3. The mean organic nitrates simulated in the BASE case agree well with observed concentrations in the boundary layer, with a bias of +10–20%, whereas a small negative bias may have been expected as a result of the previously discussed underestimate of MVK+MACR (Figure 1). The model underestimates free tropospheric  $\Sigma\text{ANs}$  by about a factor of 3. The correlation of ozone with  $\Sigma\text{ANs}$  provides an additional means of evaluating organic nitrate abundances because both organic nitrates and ozone are produced from the reactions of  $\text{RO}_2$  radicals with NO, so the concentration ratio may normalize for any model errors in the absolute concentrations of  $\text{RO}_2$  or in the rate of boundary layer

ventilation. The BASE model reproduces the observed  $\Delta\text{O}_3/\Delta\Sigma\text{AN}$  correlation slope (81.0 simulated, 81.7 observed), although the correlation is much stronger in the model ( $r^2 = 0.76$  versus 0.12 observed). This slope is similar to the relationship reported by *Day et al.* [2003] for a rural location in California and to those reported by *Rosen et al.* [2004] and *Cleary et al.* [2005] for urban areas in late afternoon. Using the methodology of *Rosen et al.* [2004] and *Cleary et al.* [2005], a  $\Delta\text{O}_3/\Delta\Sigma\text{AN}$  slope of 81.7 corresponds to an “effective  $\Sigma\text{AN}$  yield” of 2.4% from the complete mix of ozone-producing VOCs. An “effective  $\Sigma\text{AN}$  yield” of about a factor of two lower than the yield calculated from OH-initiated VOC chemistry (dominated here by isoprene) in the daytime is similar to results reported by *Rosen et al.* [2004] and *Cleary et al.* [2005]. The 8% simulation overestimates  $\Sigma\text{ANs}$  (+40% bias) and underestimates the  $\Delta\text{O}_3/\Delta\Sigma\text{AN}$  slope (62.8).

[27] The simulations with slower photochemical loss of ONITR (4%\_slowCHEM and 8%\_slowCHEM) have only slightly (+5–6%) higher boundary layer concentrations (Figure 3) and burdens (Table 2) of  $\Sigma\text{ANs}$  than the corresponding simulations with the faster ONITR + OH reaction rate, even though the ozone and OH reaction rate constants were decreased by about a factor of 3. This small response reflects the much larger contribution to  $\Sigma\text{ANs}$  from secondary multifunctional nitrates (XNITR, accounting for 92% of  $\Sigma\text{ANs}$  in BASE) than from primary isoprene nitrates (ONITR). In the 4%\_slowCHEM simulation, the burden of ONITR (which has photochemical losses) increases by a factor of 2.5 versus BASE, but XNITR (which is produced from ONITR, but lost only by export and deposition) decreases by –7.4%. The higher concentrations of  $\Sigma\text{ANs}$  decrease the  $\Delta\text{O}_3/\Delta\Sigma\text{AN}$  correlation slope slightly, with little impact on mean concentrations (Figure 3).

[28] When the reactions of ONITR with ozone and OH are allowed to recycle all of the  $\text{NO}_x$  (4%\_100% $\text{NO}_x$ ), boundary layer concentrations of  $\Sigma\text{ANs}$  are underestimated by a factor of 6 or more. If we additionally assume an 8% yield of ONITR and slow photochemical loss, the  $\Sigma\text{AN}$  concentrations increase, but are still a factor of 2.5–4 below observed values, and the  $\Delta\text{O}_3/\Delta\Sigma\text{AN}$  correlation slope is still greatly overestimated (252.0). In both of the simulations with 100% recycling (4%\_100% $\text{NO}_x$ , 8%\_slowCHEM\_100% $\text{NO}_x$ ), free tropospheric  $\Sigma\text{AN}$  concentrations are dramatically underestimated by a factor of 15 or more. On the other hand, if the ONITR reactions with OH and ozone are assumed to recycle no  $\text{NO}_x$  (4%\_0% $\text{NO}_x$ ), instead forming XNITR exclusively,  $\Sigma\text{AN}$  concentrations increase by over 50% from the BASE case, leading to 70% overestimates of observed boundary layer  $\Sigma\text{ANs}$  and a large underestimate of  $\Delta\text{O}_3/\Delta\Sigma\text{AN}$  (50.7).

[29] In the final set of sensitivity simulation, the dry deposition velocity of isoprene nitrates is decreased from that of  $\text{HNO}_3$  to that of PAN (simulations 4%\_slowDD and 8%\_slowDD). In these simulations,  $\Sigma\text{AN}$  concentrations increase by approximately a factor of 2, dramatically worsening agreement with observed  $\Sigma\text{AN}$  concentrations and  $\Delta\text{O}_3/\Delta\Sigma\text{AN}$  correlation slopes in the boundary layer; simulated concentrations of  $\Sigma\text{ANs}$  in the free troposphere approach observed values, but are still slightly underesti-

ated. The discrepancy between simulated and observed  $\Sigma\text{ANs}$  in the free troposphere is discussed further below.

[30] From the comparisons with observed boundary layer  $\Sigma\text{ANs}$  and  $\Delta\text{O}_3/\Delta\Sigma\text{AN}$ , we find that the BASE and 4%\_slowCHEM simulations — with a 4% yield of isoprene nitrates from ISOPO<sub>2</sub>+NO, recycling of 40%  $\text{NO}_x$ , and fast loss by dry deposition — best match observations of  $\Sigma\text{AN}$  concentrations and  $\Delta\text{O}_3/\Delta\Sigma\text{AN}$  correlation slopes. The simulations with an 8% yield degrade agreement with observation somewhat. The simulations with slow dry deposition and those with either 0% or 100%  $\text{NO}_x$  recycling show the worst agreement with observations. On the basis of these results, we select the BASE and 4%\_slowCHEM cases as the “best guess” set of model parameters, but also consider a range of uncertainty including the other simulations showing reasonable agreement (within  $\sim\pm 50\%$ ) with observations (8%, 8%\_slowCHEM).

[31] Our best guess of a 4% yield of isoprene nitrates agrees well with the values measured by *Chen et al.* [1998], but is significantly lower than the values (up to 15%) from other studies [*Tuazon and Atkinson*, 1990; *Chuong and Stevens*, 2002; *Sprengnether et al.*, 2002]. The BASE case rate constants for isoprene nitrate loss with OH and ozone are within the range estimated by *Giacopelli et al.* [2005], but we find that the agreement with observations is only slightly degraded using slower reaction rates [e.g., *Paulson and Seinfeld*, 1992; *Chen et al.*, 1998]. We find that the assumption of 40%  $\text{NO}_x$  recycling from ONITR+OH gives the best agreement with observations, although a somewhat higher recycling rate could be supported, especially if the production yield of isoprene nitrates were higher. The degree of recycling has not been well constrained by previous studies, with *Paulson and Seinfeld* [1992] arguing that  $\text{NO}_x$  should be released from this reaction, but other studies suggesting the formation of secondary multifunctional nitrates [*Grossenbacher et al.*, 2001; *Giacopelli et al.*, 2005]. Finally, our results suggest that isoprene nitrates are removed relatively quickly by dry deposition, as supported by observations from *Rosen et al.* [2004] and *Horii et al.* [2006], but faster than suggested by *Shepson et al.* [1996] and *Giacopelli et al.* [2005].

[32] Most of the analysis in this paper has focused on the chemistry of the continental boundary layer, where short-lived isoprene is abundant and isoprene nitrates are expected to dominate  $\Sigma\text{ANs}$ . In the boundary layer, we find that the BASE simulation best reproduces the ICARTT observations of  $\Sigma\text{AN}$  concentrations and  $\Delta\text{O}_3/\Delta\Sigma\text{AN}$  correlations. All of the simulations presented here, however, considerably underestimate  $\Sigma\text{ANs}$  in the free troposphere. The speciated alkyl nitrates measured during ICARTT typically account for only  $\sim 10\%$  of the observed  $\Sigma\text{ANs}$  even in the free troposphere, suggesting that the missing species are larger or multifunctional nitrates. In the BASE simulation, which underestimates free tropospheric  $\Sigma\text{AN}$  concentrations by a factor of 3, secondary multifunctional nitrates (XNITR) contribute over 90% of the simulated total. The simulations that most closely match the free tropospheric observations (4%\_slowDD and 8%\_slowDD; mean biases of –40% and –25%, respectively) overestimate  $\Sigma\text{ANs}$  by factors of 2–3 (and underestimate the  $\Delta\text{O}_3/\Delta\Sigma\text{AN}$  correlation slope by a factor of 2 or more) in the

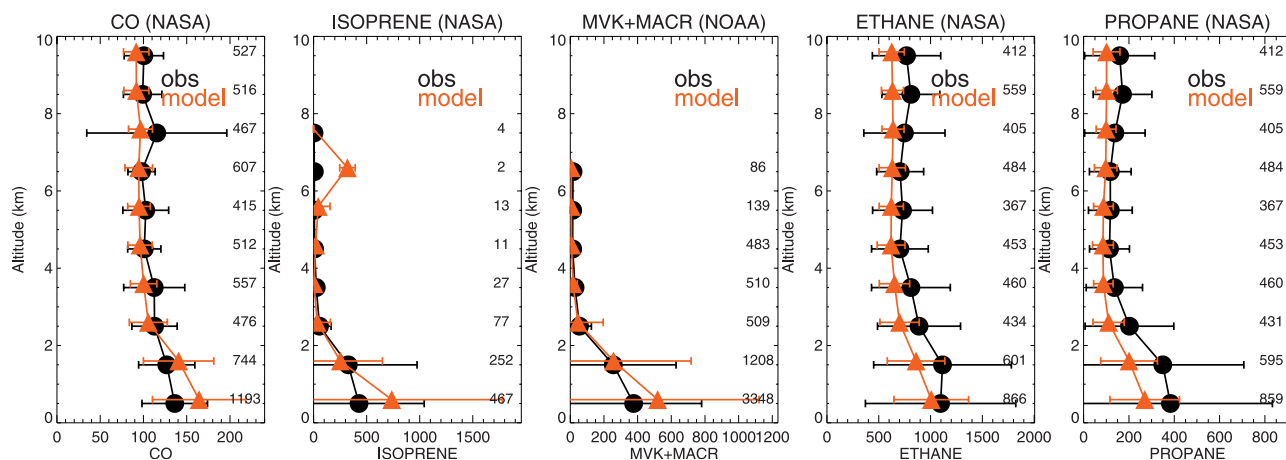


**Figure 4.** Mean ICARTT vertical profiles of CO, isoprene, methylvinyl ketone + methacrolein, ethane, and propane from observations on the NASA DC-8 and NOAA WP-3D (black, standard deviations indicated by horizontal bars) and model sampled along the appropriate flight tracks (red). Hourly model results are sampled at the locations of the 1-min observations.

boundary layer. The simulations with 100%  $\text{NO}_x$  recycling (and no XNITR production) from ONITR + OH (4%\_100%NO<sub>x</sub> and 8%\_slowCHEM\_100%NO<sub>x</sub>) underestimate free tropospheric concentrations by a factor of 15 or more. From the strong correlation between isoprene nitrate export from the boundary layer (Figure 2) and free tropospheric  $\Sigma\text{AN}$  concentrations (Figure 3) in our model, we estimate that a monthly export flux of  $\sim 50$  GgN could enable the model to reproduce observed free tropospheric  $\Sigma\text{AN}$ s.

[33] Possible causes of the underestimate of  $\Sigma\text{AN}$ s in all simulations include insufficient vertical mixing or other sources of organic nitrates in the free troposphere not represented in the model. Insufficient vertical mixing out of the boundary layer could also account for the model overestimate of  $\text{NO}_x$  and CO in Figure 1. While increased boundary layer ventilation would decrease isoprene nitrate concentrations in the boundary layer, it would not be expected to alter the simulated ratio  $\Delta\text{O}_3/\Delta\Sigma\text{AN}$  dramatically, suggesting that constraints derived above from boundary layer observations should be robust to a possible model bias in ventilation. High isoprene nitrate export only occurs in our simulations, however, when boundary layer  $\Sigma\text{AN}$  concentrations are strongly overestimated. In Figure 4, we evaluate the boundary layer ventilation in the model by comparing simulated and observed vertical profiles of several hydrocarbons with strong boundary layer sources (and their oxidation products). Since the vertical gradients of these species have no systematic bias, we find little evidence of insufficient boundary layer ventilation in the model. Instead, the bias appears to be due to a missing source of organic nitrates in the free troposphere. For instance, subsequent steps in the oxidation of monoterpenes or other hydrocarbons, not adequately represented in our mechanism, could lead to further production of organic nitrates. Also, our model treats both aldehydic and hydroxy nitrates as a single species, whereas less efficient removal of the aldehydic nitrates by wet and dry deposition could increase export and improve the simulation of free tropospheric  $\Sigma\text{AN}$ s.

### 4.3. Implications for $\text{NO}_x$ Budget

[34] We find that the formation of isoprene nitrates has a large effect on the  $\text{NO}_x$  budget in the summertime boundary layer (Figure 2). In the BASE simulation, which best agrees with the  $\Sigma\text{AN}$  and  $\Delta\text{O}_3/\Delta\Sigma\text{AN}$  observations in the boundary layer (Figure 3), out of a total 519 GgN surface  $\text{NO}_x$  emissions from the eastern United States in July, 79 GgN (15% of emissions) cycles through isoprene nitrates. Once formed, 27 GgN (5% of emissions) is recycled from isoprene nitrates back to  $\text{NO}_x$  within the continental boundary layer, 39 GgN (8% of emissions) are removed permanently by dry and wet deposition, and 13 GgN (2% of emissions) are exported to the free troposphere as isoprene nitrates. For comparison, Horowitz *et al.* [1998] estimated that isoprene nitrate net chemical production (production minus loss from recycling) accounted for 16% of  $\text{NO}_x$  emissions the eastern United States in summer, with deposition and export of isoprene nitrates equal to 14% and 1.5%, respectively. As discussed in section 4.2, a much larger export of  $\Sigma\text{AN}$ s from the boundary layer (equal to  $\sim 10\%$  of  $\text{NO}_x$  emissions) would be required to match the free tropospheric observations of  $\Sigma\text{AN}$ s (assuming no other free tropospheric source of  $\Sigma\text{AN}$ s).

[35] We estimate a range for the values above by considering those simulations that agree best with boundary layer observations of  $\Sigma\text{AN}$ s and  $\Delta\text{O}_3/\Delta\Sigma\text{AN}$  (Figure 3), excluding the simulations with slow dry deposition and with 0% and 100%  $\text{NO}_x$  recycling. We thus estimate an observationally constrained isoprene nitrate budget range of production (79–96 GgN), recycling to  $\text{NO}_x$  (23–33 GgN), deposition (39–51 GgN), and export (13–16 GgN). Note that this constrained budget range is considerably narrower than the range that would be obtained if all sensitivity simulations were considered, especially for the loss terms. The full range of losses is recycling to  $\text{NO}_x$  (0–73 GgN, 0–14% of  $\text{NO}_x$  emissions), deposition (10–57 GgN, 2–11%), and export (2–41 GgN, 0.5–8%). The full range of isoprene nitrate production (76–100 GgN, 15–19% of emissions) is similar to the constrained range above.

[36] Isoprene nitrate chemistry affects ozone concentrations through its impact on the  $\text{NO}_x$  budget. Uncertainties in the isoprene nitrate chemistry can alter the mean ozone mixing ratios in the boundary layer by up to +3.0 ppbv (in simulation 4%\_100NO<sub>x</sub>) and -2.0 ppbv (4%\_0NO<sub>x</sub>) from their BASE case values (Figure 1), demonstrating that recycling of  $\text{NO}_x$  from isoprene nitrates can have a 5 ppbv impact on ozone. If we consider only the observationally constrained simulations, the uncertainty range of mean ozone decreases to -1.4 to 0 ppbv from the BASE case.

## 5. Conclusions

[37] We combine model simulations and observations from the ICARTT field campaign over the eastern United States during summer 2004 to constrain the chemistry of isoprene nitrates. Simulated concentrations of trace species generally match observations to within 30% in the U.S. boundary layer, except for  $\text{NO}_x$  (overestimated by ~30%) and PAN (overestimated by a factor of ~2); free tropospheric concentrations of these species do not show this overestimate. Comparisons of simulated tracer vertical profiles with observations suggest that the model adequately represents boundary layer ventilation. Additional simulations are conducted to examine the sensitivity of model results to assumptions about the following uncertain aspects of isoprene chemistry: isoprene nitrate production yield, chemical loss rate,  $\text{NO}_x$  recycling, and dry deposition. Observed concentrations of total hydroxyalkyl- and alkyl-nitrates ( $\Sigma\text{ANs}$ ) and the correlation of ozone with  $\Sigma\text{ANs}$  are used to constrain the possible values of the above parameters. We find that our simulations with low deposition velocities for isoprene nitrates produce unacceptably high boundary layer concentrations of  $\Sigma\text{ANs}$ . Extreme rates of  $\text{NO}_x$  recycling (0% or 100%) from the reactions of isoprene nitrates with OH and ozone lead to  $\Sigma\text{AN}$  concentrations that are strongly biased (high or low, respectively) compared with observations, but model results are relatively insensitive to the rate of this reaction. Finally, better agreement is obtained with a lower isoprene nitrate production yield of 4% than with a higher yield of 8%. The observations are best reproduced by the BASE and 4%\_slowCHEM simulations, which match the mean observed  $\Sigma\text{AN}$  concentrations in the boundary layer within 10–20%, and the observed  $\Delta\text{O}_3/\Delta\Sigma\text{AN}$  correlation slope (81.0 and 78.4 respectively in the model, 81.7 in the observations).

[38] Our evaluation of model results versus boundary layer observations suggests that the most likely values for the parameters considered are an isoprene nitrate yield from  $\text{ISOPO}_2 + \text{NO}$  of 4%, recycling of about half of ONITR to  $\text{NO}_x$  in the reactions with OH and ozone, and fast removal of isoprene nitrates by dry deposition (at a rate similar to that of  $\text{HNO}_3$ ). We also identify a range of plausible values for these parameters based on other simulations (4%\_slowCHEM, 8%, 8%\_slowCHEM). That is, slower loss of isoprene nitrates by reaction with ozone and OH produces a negligible change in results, while an 8% yield of isoprene nitrates slightly degrades agreement with observations, but cannot be ruled out. Of course, the set of sensitivity experiments conducted here are not exhaustive of all possible values and combinations of the parameters. For example, an 8% production yield of ONITR from  $\text{ISOPO}_2 + \text{NO}$  together

with a somewhat higher rate of  $\text{NO}_x$  recycling might match observational constraints as well as the BASE simulation. This possibility for cancellation of errors in our model suggests the need for further laboratory and field studies of the chemistry and deposition rates of isoprene nitrates.

[39] We find that the  $\text{NO}_3$  production pathway accounts for 49% of the total organic nitrate production in the BASE case (with a range of ~40–50% in the observationally constrained simulations, depending on the production yield of ONITR from  $\text{ISOPO}_2 + \text{NO}$ ), qualitatively agreeing with the observational estimates of *Starn et al.* [1998]. The loss of isoprene nitrates occurs primarily by dry deposition (~45%). Reactions with ozone and OH are responsible for 24% and 10%, respectively, of the isoprene nitrate loss in BASE. In simulations with slower photochemical loss rates, these losses decrease to ~21% from ozone and ~8% from OH.

[40] Isoprene nitrates are shown to have a major impact on the  $\text{NO}_x$  budget in the summertime U.S. boundary layer. In our model simulations matching the constraints from boundary layer observations, formation of isoprene nitrates consumes 15–19% of the emitted  $\text{NO}_x$  (15% in the BASE simulation). Of this amount, deposition of isoprene nitrates permanently removes 8–10% of  $\text{NO}_x$  emissions (8% in BASE), 2–3% are exported (2% in BASE), and 4–6% are recycled to  $\text{NO}_x$  (5% in BASE). The observed free tropospheric  $\Sigma\text{AN}$  concentrations could be matched by the model if the export of nitrates were increased to ~10% of  $\text{NO}_x$  emissions. Through their impact on  $\text{NO}_x$ , isoprene nitrates also affect surface ozone concentrations. The observational constraints serve to narrow the uncertainty of this impact on ozone from 5.0 ppbv (varying from -2.0 to +3.0 ppbv from the BASE case values) to 1.4 ppbv (-1.4 to 0 ppbv from BASE).

[41] While we used available observations to constrain uncertainties in isoprene nitrate chemistry, many uncertainties still exist and require further investigation. Our model budgets indicate that the reaction of isoprene with  $\text{NO}_3$  is the major pathway for isoprene nitrate formation, but this pathway remains highly uncertain. The  $\text{NO}_3$  pathway has not typically been considered important for isoprene because of the diurnal anticorrelation between isoprene (which peaks during midday) and  $\text{NO}_3$  (which peaks at night). Since this pathway produces organic nitrates with a much higher yield than the OH pathway (in our mechanism, ~80% yield versus 4–8% for the OH pathway), however, it contributes significantly to isoprene nitrate production even though it is only a minor pathway for isoprene loss (~6% in our model). In our model, the rate of the isoprene +  $\text{NO}_3$  reaction peaks in the hours after sunset, when  $\text{NO}_3$  concentrations are increasing and isoprene concentrations are decreasing following the cessation of emissions. The degree of importance of this pathway for organic nitrate formation is sensitive, however, to the details of the diurnal cycles of isoprene emissions and OH and  $\text{NO}_3$  concentrations. We also find that our model results are highly sensitive to the degree of recycling of  $\text{NO}_x$  from the reaction of isoprene nitrates with OH and ozone. The amount of  $\text{NO}_x$  produced from these reactions, and the nature and fate of the multifunctional organic nitrates formed, need further investigation. Finally, the large discrepancy between simulated and observed  $\Sigma\text{ANs}$  in the free troposphere suggests a

shortcoming in the representation of the chemistry of organic nitrates and/or their export in the model. Available measurements are insufficient to determine whether these “missing” nitrates are isoprene nitrates or nitrates derived from other parent hydrocarbons.

[42] **Acknowledgments.** We would like to thank our colleagues H. Yang, J. Austin, and J. Orlando for their comments on this work. Three anonymous reviewers also helped to improve the paper significantly. This work benefited from helpful conversations with D. Farmer. We also thank the many ICARTT investigators who generously shared their data with us.

## References

- Andreae, M. O., and P. Merlet (2001), Emissions of trace gases and aerosols from biomass burning, *Global Biogeochem. Cycles*, *15*, 955–966.
- Aschmann, S. M., R. Atkinson, and J. Arey (2002), Products of reaction of OH radicals with  $\alpha$ -pinene, *J. Geophys. Res.*, *107*(D14), 4191, doi:10.1029/2001JD001098.
- Bey, I., D. J. Jacob, R. M. Yantosca, J. A. Logan, B. D. Field, A. M. Fiore, Q. Li, H. Y. Liu, L. J. Mickley, and M. G. Schultz (2001), Global modeling of tropospheric chemistry with assimilated meteorology: Model description and evaluation, *J. Geophys. Res.*, *106*, 23,073–23,095.
- Blake, N. J., et al. (2003), NMHCs and halocarbons in Asian continental outflow during the Transport and Chemical Evolution over the Pacific (TRACE-P) Field Campaign: Comparison With PEM-West B, *J. Geophys. Res.*, *108*(D20), 8806, doi:10.1029/2002JD003367.
- Brasseur, G. P., D. A. Hauglustaine, S. Walters, P. J. Rasch, J.-F. Müller, C. Granier, and X. X. Tie (1998), MOZART, a global chemical transport model for ozone and related chemical tracers: 1. Model description, *J. Geophys. Res.*, *103*, 28,265–28,289.
- Chen, X., D. Hulbert, and P. B. Shepson (1998), Measurement of the organic nitrate yield from OH reaction with isoprene, *J. Geophys. Res.*, *103*(D19), 25,563–25,568.
- Chuong, B., and P. S. Stevens (2002), Measurements of the kinetics of the OH-initiated oxidation of isoprene, *J. Geophys. Res.*, *107*(D13), 4162, doi:10.1029/2001JD000865.
- Cleary, P. A., J. G. Murphy, P. J. Wooldridge, D. A. Day, D. B. Millet, M. McKay, A. H. Goldstein, and R. C. Cohen (2005), Observations of total alkyl nitrates within the Sacramento Urban Plume, *Atmos. Chem. Phys. Disc.*, *5*, 4801–4843.
- Crounse, J. D., K. A. McKinney, A. J. Kwan, and P. O. Wennberg (2006), Measurement of gas-phase hydroperoxides by chemical ionization mass spectrometry, *Anal. Chem.*, *78*(19), 6726–6732, doi:10.1021/ac0604235.
- Day, D. A., P. J. Wooldridge, M. Dillon, J. A. Thornton, and R. C. Cohen (2002), A thermal dissociation-laser induced fluorescence instrument for in situ detection of NO<sub>2</sub>, peroxy(acyl)nitrates, alkyl nitrates, and HNO<sub>3</sub>, *J. Geophys. Res.*, *107*(D6), 4046, doi:10.1029/2001JD000779.
- Day, D. A., M. B. Dillon, P. J. Wooldridge, J. A. Thornton, R. S. Rosen, E. C. Wood, and R. C. Cohen (2003), On alkyl nitrates, O<sub>3</sub>, and the “missing NO<sub>x</sub>,” *J. Geophys. Res.*, *108*(D16), 4501, doi:10.1029/2003JD003685.
- de Gouw, J. A., P. D. Goldan, C. Warneke, W. C. Kuster, J. M. Roberts, M. Marchewka, S. B. Bertman, A. A. P. Pszenny, and W. C. Keene (2003), Validation of proton transfer reaction-mass spectrometry (PTR-MS) measurements of gas-phase organic compounds in the atmosphere during the New England Air Quality Study (NEAQS) in 2002, *J. Geophys. Res.*, *108*(D21), 4682, doi:10.1029/2003JD003863.
- de Gouw, J. A., et al. (2006), Volatile organic compounds composition of merged and aged forest fire plumes from Alaska and western Canada, *J. Geophys. Res.*, *111*, D10303, doi:10.1029/2005JD006175.
- Emmons, L. K., et al. (2006), Sensitivity of chemical budgets to meteorology in MOZART-4, *Eos Trans. AGU*, *87*(52), Fall Meet. Suppl., Abstract A51C-0094.
- Fan, J., and R. Zhang (2004), Atmospheric oxidation mechanism of isoprene, *Environ. Chem.*, *1*, 140–149, doi:10.1071/EN04045.
- Fehsenfeld, F. C., et al. (2006), International Consortium for Atmospheric Research on Transport and Transformation (ICARTT): North America to Europe—Overview of the 2004 summer field study, *J. Geophys. Res.*, *111*, D23S01, doi:10.1029/2006JD007829.
- Fiore, A. M., L. W. Horowitz, D. W. Purves, H. Levy II, M. J. Evans, Y. Wang, Q. Li, and R. M. Yantosca (2005), Evaluating the contribution of changes in isoprene emissions to surface ozone trends over the eastern United States, *J. Geophys. Res.*, *110*, D12303, doi:10.1029/2004JD005485.
- Frost, G. J., et al. (2006), Effects of changing power plant NO<sub>x</sub> emissions on ozone in the eastern United States: Proof of concept, *J. Geophys. Res.*, *111*, D12306, doi:10.1029/2005JD006354.
- Giapopelli, P., K. Ford, C. Espada, and P. B. Shepson (2005), Comparison of the measured and simulated isoprene nitrate distributions above a forest canopy, *J. Geophys. Res.*, *110*, D01304, doi:10.1029/2004JD005123.
- Grossenbacher, J. W., et al. (2001), Measurements of isoprene nitrates above a forest canopy, *J. Geophys. Res.*, *106*(D20), 24,429–24,438.
- Guenther, A., T. Karl, P. Harley, C. Wiedinmyer, P. I. Palmer, and C. Geron (2006), Estimates of global terrestrial isoprene emissions using MEGAN (Model of Emissions of Gases and Aerosols from Nature), *Atmos. Chem. Phys.*, *6*, 3181–3210.
- Hao, W. M., and M.-H. Liu (1994), Spatial and temporal distribution of tropical biomass burning, *Global Biogeochem. Cycles*, *8*, 495–503.
- Holloway, J. S., R. O. Jakoubek, D. D. Parrish, C. Gerbig, A. Volz-Thomas, S. Schmitgen, A. Fried, B. Wert, B. Henry, and J. R. Drummond (2000), Airborne intercomparison of vacuum ultraviolet fluorescence and tunable diode laser absorption measurements of tropospheric carbon monoxide, *J. Geophys. Res.*, *105*, 24,251–24,262.
- Horii, C. V., J. W. Munger, S. C. Wofsy, M. Zahniser, D. Nelson, and J. B. McManus (2006), Atmospheric reactive nitrogen concentration and flux budgets at a northeastern U.S. forest site, *Agric. For. Meteorol.*, *136*, 159–174.
- Horowitz, L. W., J. Liang, G. M. Gardner, and D. J. Jacob (1998), Export of reactive nitrogen from North America during summertime: Sensitivity to hydrocarbon chemistry, *J. Geophys. Res.*, *103*, 13,451–13,476.
- Horowitz, L. W., et al. (2003), A global simulation of tropospheric ozone and related tracers: Description and evaluation of MOZART, version 2, *J. Geophys. Res.*, *108*(D24), 4784, doi:10.1029/2002JD002853.
- Houweling, S., F. Dentener, and J. Lelieveld (1998), The impact of non-methane hydrocarbon compounds on tropospheric photochemistry, *J. Geophys. Res.*, *103*, 10,673–10,696.
- Kwok, E. S. C., and R. Atkinson (1995), Estimation of hydroxyl radical reaction rate constants for gas-phase organic compounds using a structure-reactivity relationship: An update, *Atmos. Environ.*, *29*, 1685–1695.
- Madronich, S., and S. Flocke (1998), The role of solar radiation in atmospheric chemistry, in *Handbook of Environmental Chemistry*, edited by P. Boule, pp. 1–26, Springer, New York.
- McLinden, C. A., S. C. Olsen, B. Hannegan, O. Wild, M. J. Prather, and J. Sundet (2000), Stratospheric ozone in 3-D models: A simple chemistry and the cross-tropopause flux, *J. Geophys. Res.*, *105*, 14,653–14,665.
- Müller, J.-F. (1992), Geographical distribution and seasonal variation of surface emissions and deposition velocities of atmospheric trace gases, *J. Geophys. Res.*, *97*, 3787–3804.
- Neeb, P. (2000), Structure-reactivity based estimation of the rate constants for hydroxyl radical reactions with hydrocarbons, *J. Atmos. Chem.*, *35*, 295–315.
- Nozière, B., I. Barnes, and K. Becker (1999), Product study and mechanisms of the reactions of  $\alpha$ -pinene and of pinonaldehyde with OH radicals, *J. Geophys. Res.*, *104*(D19), 23,645–23,656.
- O'Brien, J. M., P. B. Shepson, K. Muthuramu, C. Hau, H. Niki, D. R. Hastie, R. Taylor, and P. B. Roussel (1995), Measurement of alkyl and multifunctional organic nitrates at a rural site in Ontario, *J. Geophys. Res.*, *100*, 22,795–22,804.
- Olivier, J., J. Peters, C. Granier, G. Pétron, J. F. Müller, and S. Wallens (2003), Present and future surface emissions of atmospheric compounds, *POET Rep. 2, EU Proj. EVK2-1999-00011*.
- Paulson, S. E., and J. H. Seinfeld (1992), Development and evaluation of a photooxidation mechanism for isoprene, *J. Geophys. Res.*, *97*, 20,703–20,715.
- Paulson, S. E., R. C. Flagan, and J. H. Seinfeld (1992), Atmospheric photooxidation of isoprene part I: The hydroxyl radical and ground state atomic oxygen reactions, *Int. J. Chem. Kinet.*, *24*, 79–101.
- Pöschl, U., R. von Kuhlmann, N. Poisson, and P. J. Crutzen (2000), Development and intercomparison of condensed isoprene oxidation mechanisms for global atmospheric modeling, *J. Atmos. Chem.*, *37*, 29–52.
- Roller, C., A. Fried, J. Walega, P. Weibring, and F. Tittel (2006), Advances in hardware, system diagnostics software, and acquisition procedures for high performance airborne tunable diode laser measurements of formaldehyde, *Appl. Phys. B*, *82*, 247–264, doi:10.1007/s00340-005-1998-8.
- Rosen, R. S., E. C. Wood, P. J. Wooldridge, J. A. Thornton, D. A. Day, W. Kuster, E. J. Williams, B. T. Jobson, and R. C. Cohen (2004), Observations of total alkyl nitrates during Texas Air Quality Study 2000: Implications for O<sub>3</sub> and alkyl nitrate photochemistry, *J. Geophys. Res.*, *109*, D07303, doi:10.1029/2003JD004227.
- Ryerson, T. B., et al. (2003), Effect of petrochemical industrial emissions of reactive alkenes and NO<sub>x</sub> on tropospheric ozone formation in Houston, Texas, *J. Geophys. Res.*, *108*(D8), 4249, doi:10.1029/2002JD003070.
- Sachse, G. W., G. F. Hill, L. O. Wade, and M. G. Pery (1987), Fast-response, high-precision carbon monoxide sensor using a tunable diode laser absorption technique, *J. Geophys. Res.*, *92*, 2071–2081.

- Shepson, P. B., E. Mackay, and K. Muthuramu (1996), Henry's law constants and removal processes for several atmospheric  $\beta$ -hydroxy alkyl nitrates, *Environ. Sci. Technol.*, *30*, 3618–3623.
- Sillman, S., and P. J. Samson (1995), Impact of temperature on oxidant photochemistry in urban, polluted rural and remote environments, *J. Geophys. Res.*, *100*(D6), 11,497–11,508.
- Singh, H., et al. (2000), Distribution and fate of selected oxygenated organic species in the troposphere and lower stratosphere over the Atlantic, *J. Geophys. Res.*, *105*(D3), 3795–3806.
- Singh, H. B., W. H. Brune, J. H. Crawford, D. J. Jacob, and P. B. Russell (2006), Overview of the summer 2004 Intercontinental Chemical Transport Experiment–North America (INTEX-A), *J. Geophys. Res.*, *111*, D24S01, doi:10.1029/2006JD007905.
- Singh, H. B., et al. (2007), Reactive nitrogen distribution and partitioning in the North American troposphere and lowermost stratosphere, *J. Geophys. Res.*, *112*, D12S04, doi:10.1029/2006JD007664.
- Slusher, D. L., L. G. Huey, D. J. Tanner, F. M. Flocke, and J. M. Roberts (2004), A thermal dissociation-chemical ionization mass spectrometry (TD-CIMS) technique for the simultaneous measurement of peroxyacyl nitrates and dinitrogen pentoxide, *J. Geophys. Res.*, *109*, D19315, doi:10.1029/2004JD004670.
- Sprengnether, M., K. L. Demerjian, N. M. Donahue, and J. G. Anderson (2002), Product analysis of the OH oxidation of isoprene and 1,3-butadiene in the presence of NO, *J. Geophys. Res.*, *107*(D15), 4268, doi:10.1029/2001JD000716.
- Starn, T. K., P. B. Shepson, S. B. Bertman, D. D. Riemer, R. G. Zika, and K. Olszyna (1998), Nighttime isoprene chemistry at an urban-impacted forest site, *J. Geophys. Res.*, *103*(D17), 22,437–22,448.
- Thornton, J. A., P. J. Wooldridge, and R. C. Cohen (2000), Atmospheric NO<sub>2</sub>: In situ laser-induced fluorescence detection at parts per trillion mixing ratios, *Anal. Chem.*, *72*, 528–539, doi:10.1021/ac9908905.
- Tie, X., S. Madronich, S. Walters, D. P. Edwards, P. Ginoux, N. Mahowald, R. Zhang, C. Lou, and G. Brasseur (2005), Assessment of the global impact of aerosols on tropospheric oxidants, *J. Geophys. Res.*, *110*, D03204, doi:10.1029/2004JD005359.
- Trainer, M., E. J. Williams, D. D. Parrish, M. P. Buhr, E. J. Allwine, H. H. Westberg, F. C. Fehsenfeld, and S. C. Liu (1987), Models and observations of the impact of natural hydrocarbons on rural ozone, *Nature*, *329*, 705–707.
- Trainer, M., et al. (1991), Observations and modeling of the reactive nitrogen photochemistry at a rural site, *J. Geophys. Res.*, *96*(D2), 3045–3063.
- Treves, K., and Y. Rudich (2003), The atmospheric fate of C<sub>3</sub>–C<sub>6</sub> hydroxyalkyl nitrates, *J. Phys. Chem. A*, *107*, 7809–7817.
- Tuazon, E. C., and R. Atkinson (1990), A product study of the gas-phase reaction of isoprene with the OH radical in the presence of NO<sub>x</sub>, *Int. J. Chem. Kinet.*, *22*, 1221–1236.
- Turnipseed, A. A., L. G. Huey, E. Nemitz, R. Stickel, J. Higgs, D. J. Tanner, D. L. Slusher, J. P. Sparks, F. Flocke, and A. Guenther (2006), Eddy covariance fluxes of peroxyacetyl nitrates (PANs) and NO<sub>y</sub> to a coniferous forest, *J. Geophys. Res.*, *111*, D09304, doi:10.1029/2005JD006631.
- Turquetly, S., et al. (2007), Inventory of boreal fire emissions for North America in 2004: Importance of peat burning and pyroconvective injection, *J. Geophys. Res.*, *112*, D12S03, doi:10.1029/2006JD007281.
- Vay, S. A., B. E. Anderson, G. W. Sachse, J. E. Collins Jr., J. R. Podolske, C. H. Twohy, B. Gandrud, K. R. Chan, S. L. Baughcum, and H. A. Wallio (1998), DC-8-based observations of aircraft CO, CH<sub>4</sub>, N<sub>2</sub>O, and H<sub>2</sub>O (g) emission indices during SUCCESS, *Geophys. Res. Lett.*, *25*, 1717–1720.
- von Kuhlmann, R., M. G. Lawrence, U. Pöschl, and P. J. Crutzen (2004), Sensitivities in global scale modeling of isoprene, *Atmos. Chem. Phys.*, *4*, 1–17.
- Wu, S., L. J. Mickley, D. J. Jacob, J. A. Logan, R. M. Yantosca, and D. Rind (2007), Why are there large differences between models in global budgets of tropospheric ozone?, *J. Geophys. Res.*, *112*, D05302, doi:10.1029/2006JD007801.

R. C. Cohen, A. Perring, and P. J. Wooldridge, Department of Chemistry, University of California, Berkeley, CA 94720, USA.

L. K. Emmons, P. G. Hess, and J.-F. Lamarque, Atmospheric Chemistry Division, National Center for Atmospheric Research, Boulder, CO 80305, USA.

A. M. Fiore, L. W. Horowitz, and G. P. Milly, Geophysical Fluid Dynamics Laboratory, NOAA, Princeton, NJ 08540, USA. (larry.horowitz@noaa.gov)